7-27-2006

Photoreductive dissolution of ferrihydrite by methanesulfinic acid: Evidence of a direct link between dimethylsulfide and iron-bioavailability

Anne M. Johansen

Jennifer M. Key

Photoreductive dissolution of ferrihydrite by methanesulfinic acid: Evidence of a direct link between dimethylsulfide and iron-bioavailability

Anne M. Johansen[1] and Jennifer M. Key[1]

Received 9 February 2006; revised 12 April 2006; accepted 6 June 2006; published 27 July 2006.

[1] Within open-ocean regions where excess macronutrients are present, phytoplankton growth is limited by the bioavailability of iron supplied to these areas primarily within atmospheric aerosols of crustal origin. However, processes that control the abundance of biologically accessible iron in these aerosols are largely unknown. Here we show that dissolution of ferrihydrite, a surrogate iron(oxy)hydroxide phase found in atmospheric waters, is enhanced in the presence of methanesulfinic acid (MSIA, CH_3SO_2H, a dimethylsulfide (DMS) oxidation intermediate) in laboratory irradiation experiments with aqueous suspensions that simulate marine aerosol particles. The increased release of soluble Fe(II) is attributed to a species specific and direct photochemical reduction rather than a proton-promoted effect, and suggests an efficient mechanism by which iron-starved phytoplankton can actively increase aerosol iron-bioavailability by increasing DMS emissions.
Citation: Johansen, A. M., and J. M. Key (2006), Photoreductive dissolution of ferrihydrite by methanesulfinic acid: Evidence of a direct link between dimethylsulfide and iron-bioavailability, *Geophys. Res. Lett.*, *33*, L14818, doi:10.1029/2006GL026010.

1. Introduction

[2] In large regions of the open ocean iron is a limiting growth nutrient to phytoplankton, which produce half of Earth's photosynthesis and constitute one of its largest carbon sinks [*Field et al.*, 1998; *Martin and Fitzwater*, 1988]. The main delivery pathway for iron in these regions is the deposition of atmospheric Fe(III)-bearing mineral aerosols originating from continental landmasses [*Coale et al.*, 1996; *Duce and Tindale*, 1991]. Its in-situ availability to phytoplankton is further limited to only the sub-nanomolar concentration of iron that is soluble, comprised of varying fractions of organically complexed Fe(III), dissolved inorganic Fe(III) hydrolysis species, and Fe(II) [*Shaked et al.*, 2005; *Sunda*, 2001]. Although thermodynamically unstable against oxidation in oxygen-containing waters [*Stumm and Morgan*, 1996], the more soluble Fe(II) can reach steady-state concentrations of 30–75% of the total dissolved iron pool in irradiated seawater samples in the absence of organic complexation [*Voelker and Sedlak*, 1995] and up to 58% of total iron in marine aerosol particles [*Chen and Siefert*, 2004]. An important source of this Fe(II) is from photochemical reduction of Fe(III) in ligand-to-metal-charge-transfer (LMCT) reactions such as by organic ligands with carboxylic acid moieties [*Barbeau and Moffett*, 2000; *Moffett*, 2001; *Pehkonen et al.*, 1993]. In the atmosphere, oxalate is particularly effective in enhancing Fe(II) production [*Pehkonen et al.*, 1993], but it is geographically limited to its continental source regions. The mechanisms that control iron speciation in aerosol particles over remote open-oceans have remained largely unidentified [*Chen and Siefert*, 2004; *Hand et al.*, 2004]. Here we describe an efficient and specific chemical mechanism by which concentrations of Fe(II) in aerosols can be substantially increased by DMS oxidation prior to deposition into the ocean. Although the acidification of aerosol particles associated with DMS oxidation may enhance iron dissolution [*Zhuang et al.*, 1992], the mechanism presented here does not depend on such a hypothetical pH decrease and may therefore directly link DMS emission by iron deficient phytoplankton [*Sunda et al.*, 2002] to aerosol iron bioavailability [*Sunda*, 2001; *Zhuang et al.*, 1992]. This iron-sulfur reaction also constitutes a new process for aqueous phase oxidation of DMS-derived species that may affect the formation of cloud condensation nuclei (CCN) and therefore the earth's albedo and global climate.

2. Methods

[3] Environmental conditions in aerosol particles were simulated by irradiating aqueous suspensions of synthesized ferrihydrite, an amorphous iron(oxy)hydroxide that is a likely component in processed crustal aerosol particles [*Pehkonen et al.*, 1993; *Schwertmann and Cornell*, 1991], to which methanesulfinic acid (MSIA, CH_3SO_2H) or dimethylsulfoxide (DMSO, CH_3SOCH_3) were added. Experiments were carried out in 0.100 L of 18 MΩ water in a temperature controlled (293 K) water jacketed batch reactor vessel to which the reactants were added immediately before irradiation. Solar irradiation at noon at the equator (1.2 kW m^{-2}) was simulated with an IR and Air Mass (0 and 1) filtered light beam from a 1000 W Xenon lamp. Throughout each 10-hour experiment (6 hours with and 4 hours without irradiation) aliquots were removed at set time intervals and filtered through a 0.45 μm pore-size Acrodisc® syringe filter prior to the following analyses: (i) Fe(II) by complexation with ferrozine and absorbance at 562 nm in a 1 cm Z-cell (FIAlab Instruments, Inc.) [*Stookey*, 1970], (ii) MSIA, MSA (methanesulfonic acid, CH_3SO_3H) and SO_4^{2-} by ion chromatography with columns AG/AS11-HC (Dionex Corp.) in a gradient elution from 15 to 20 mM NaOH (11 minutes, 1.5 ml min^{-1}), and (iii) H_2O_2 with an Apollo 400-4 Channel Fee Radical Analyzer using a 100 μm H_2O_2 microprobe sensor (WPI, Inc.). The pH was deter-

[1]Department of Chemistry, Central Washington University, Ellensburg, Washington, USA.

0094-8276/06/2006GL026010

mined at times 0, 6 and 10 hours. Detection limits were established by adding to the mean of the blank 3 times the standard deviation of eight replicate samples and revealed to be 0.4 μM for Fe(II), 1.2 μM for MSIA, 0.82 μM for MSA, 7.1 μM for SO_4^{2-}, and 2.8 μM for H_2O_2 (after subtracting the background water H_2O_2 concentration of 6.2 μM). Due to the nature of the experiments it was not feasible to perform every experiment in triplicate, however, based on triplicate runs of several sets of experimental conditions involving Fe and MSIA or DMSO, the following relative standard deviations revealed good reproducibility: less than 4% for the Fe(II) data, 19% for the sulfur and H_2O_2 data, and 2% for the pH values (see Figure S1 in auxiliary material).[1]

[4] Amorphous ferrihydrite ($Fe_5HO_8 \cdot 4H_2O$, Molecular Mass of 108 per mole of Fe) was synthesized by following procedures given by *Schwertmann and Cornell* [1991]. Powder X-Ray Diffraction (XRD) scans were collected on the ground ferrihydrite before and after photochemical experiments and resembled that of a 2-line ferrihydrite. The surface area was 196 $m^2\ g^{-1}$ as determined using the BET method with N_2 gas.

[5] Initial concentrations in the reaction medium were calculated assuming a liquid water content typical of the marine boundary layer, 1×10^{-10} m^3 water $(m^3$ air$)^{-1}$ [*von Glasow and Sander*, 2001], representing 1×10^6 m^3 of air per 0.100 L of water. For ferrihydrite: assuming 25% of Fe is present as the more labile iron(oxy)hydroxide and a total Fe concentration of 525 ng m^{-3} (over the Atlantic Ocean) [*Chen and Siefert*, 2004; *Johansen et al.*, 2000], the calculated 2.35 nmol Fe m^{-3} correspond to 254 ng ferrihydrite m^{-3}; in 1×10^6 m^3 of air, i.e., 0.1 L of reaction medium, this is 0.25 g of ferrihydrite. For DMSO: 86 pptv DMSO, observed in particulate phase over the Atlantic Ocean [*Sciare et al.*, 2000], corresponds to 3.5×10^{-12} mol m^{-3}, and in 1×10^{-6} m^3 air 3.5×10^{-6} mols or 0.25 ml DMSO to 0.100 L. For MSIA: since MSIA has not been quantified in the atmosphere, an initial value was chosen that was well suited for analytical reasons; 0.13 mmols in 0.1 L, corresponding to an atmospheric particulate phase concentration of 1.3×10^{-10} mol m^{-3}.

3. Results

[6] Results for a representative data set are plotted in Figure 1 as a function of time. The initial Fe(II) photoproduction rate is enhanced by a factor of 6 in solution with MSIA compared to the light control without MSIA (circles vs. squares, Figure 1a); initial rates are 1.3×10^{-7} and 2.2×10^{-8} M s^{-1}, respectively. Concurrently, MSIA is consumed rapidly as MSA increases (circles, Figure 1b), and H_2O_2 is produced (circles, Figure 1c). Strong correlations between Fe(II), MSA and H_2O_2 productions during the initial 60 minutes demonstrate direct chemical interactions between all species (see Figure S2 in auxiliary material). Note that the initial MSIA concentration in solution with ferrihydrite is less than half (620 μM) the added MSIA due to adsorption of MSIA to ferrihydrite. This surface complex equilibrium might also explain the non-linearity between MSIA and other analytes (Figure S2).

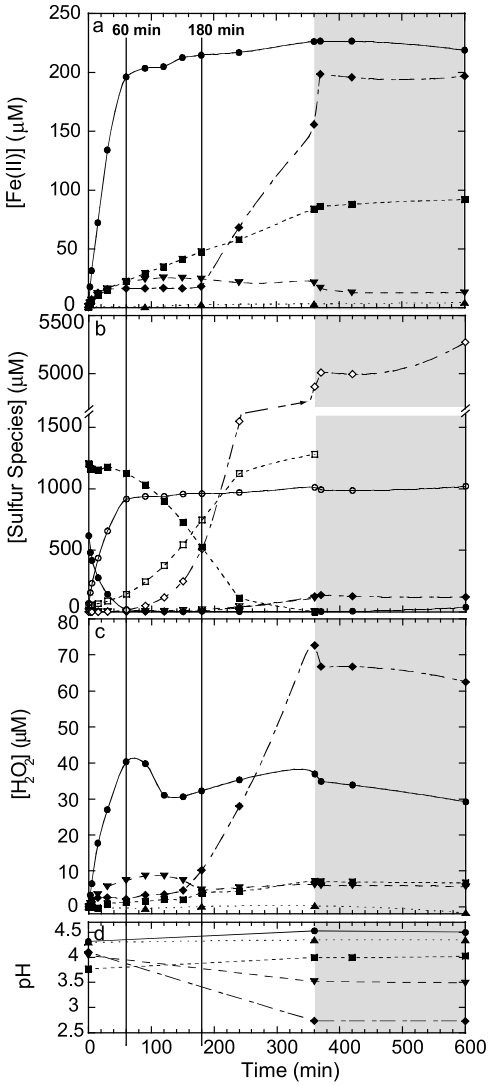

Figure 1. Photochemical experiments. Concentrations of analytes as a function of time: (a) Fe(II), (b) MSIA (solid symbols) and MSA (open symbols), (c) H_2O_2, and (d) pH. Symbols: Experiment with ferrihydrite and MSIA in the presence of light (solid circles), experiment with ferrihydrite and DMSO in the presence of light (solid downward pointing triangles), experiment with ferrihydrite and DMSO in the presence of more UV light (no AM1 filter) (solid diamonds), light control experiments (solid squares): Figure 1a with ferrihydrite only, and Figure 1b with MSIA only, dark control experiment with ferrihydrite and MSIA (solid upward pointing triangles). The light source was turned off after 360 min, plotted in the shaded area.

MSIA oxidation occurs rapidly in the presence of iron compared to the known slow photolysis of MSIA [*Bardouki et al.*, 2002] in the control (squares, Figure 1b).

[7] Significant enhancement in Fe(II) production is seen with MSIA concentrations equal to 2% of the initially added amount, corresponding to 2.6×10^{-12} mol MSIA m^{-3} air, the same order of magnitude as DMSO concentrations observed in particles [*Sciare et al.*, 2000]. Of particular importance is that enhanced Fe(II) production with MSIA is not a consequence of solution pH change; the pH increases

[1] Auxiliary material is available in the HTML. doi: 10.1029/2006GL026010.

by 0.2 units (solid circles, Figure 1d). In the control without MSIA the pH remains essentially unchanged at 4.3 (solid squares, Figure 1d).

[8] Light-induced Fe(II) formation is significantly slower in the presence of DMSO as compared to the irradiation experiment with only ferrihydrite unless DMSO is oxidized to MSIA by $OH^{\cdot}$ [*Bardouki et al.*, 2002], which is photolytically produced from traces of NO_3^- in the ferrihydrite in the experiment with higher UVR doses (inverted triangles and diamonds, Figure 1a). Once sufficient MSIA has been produced in this way, it complexes with Fe(III) and significantly enhances Fe(II) photo-production. The onset of increased Fe(II) production occurs after 180 minutes (delineated in Figure 1), when MSIA concentrations are near detection limits. At this point, MSA (Figure 1b) and H_2O_2 (Figure 1c) concentrations increase as well, analogous to the Fe-MSIA experiment. The pH drops from 4.1 to 2.7 (Figure 1d) due to the exponential increase in proton generating acids, MSIA and MSA, thus further stabilizing the newly generated Fe(II) against oxidation [*Stumm and Morgan*, 1996; *Zhuang et al.*, 1992]. Although the drop in pH could contribute to Fe(II) production in other ways, such as through increased concentrations of photoactive $FeOH^{2+}$ in solution, the differences in production rates between Fe(II) and the acids suggest that the Fe-MSIA mechanism plays a predominant role in the DMSO experiment as well.

[9] The observed lag time varied in experiments with different batches of ferrihydrite, and among those experiments with shorter lag times (see Figure S3 in auxiliary material), a leveling off of Fe(II) production was observed before completion of the experiment, alongside exponentially increasing MSIA and MSA concentrations. This indicates that mass transport to and from the surface of the particles appears to eventually limit the dissolution process, as has been observed in analogous systems involving ferrihydrite surfaces [*Stumm and Morgan*, 1996; *Wehrli et al.*, 1989] and argues for a surface- instead of a solution-photoactive complex between Fe(III) and MSIA.

4. Discussion

[10] Reaction mechanisms that help explain these observations are represented schematically in Figure 2. We suggest the initial formation of a surface complex between Fe(III) and MSIA, much in the same way that carboxylic and α-hydroxy carboxylic acid groups complex to iron (oxy)hydroxides [*Wehrli et al.*, 1989]. Structurally, the carboxylic acid (from the oxalate) and the sulfinic acid (from the MSIA) groups are very similar (equations (1) and (2), respectively) and the center C and S atoms have almost identical electronegativities (2.55 and 2.58, respectively).

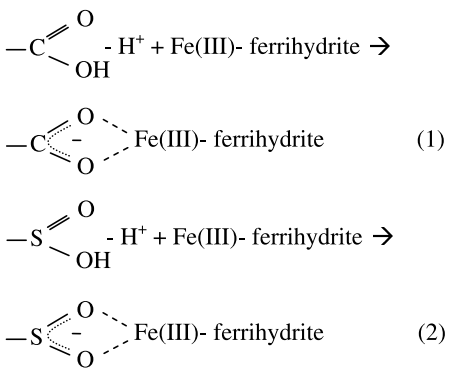

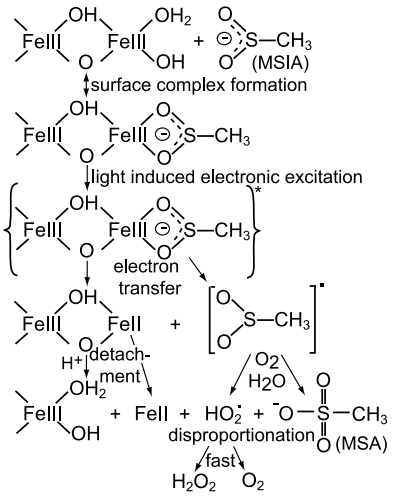

Figure 2. Schematic representation of proposed Fe(III)-MSIA LMCT mechanism.

[11] This type of surface complex involving carboxylic groups facilitates the photo-reductive dissolution of iron in a LMCT by the absorption of radiation in the visible range [*Barbeau and Moffett*, 2000; *Pehkonen et al.*, 1993; *Wehrli et al.*, 1989]. The formation of such a radiation absorbing Fe(III)-MSIA surface complex was confirmed by UV-Vis absorption spectroscopy, which showed 2 absorption bands (see Figure S4 in auxiliary material): one between wavelengths 240 and 300 nm, and the other, in the visible range of the solar spectrum, from 350 to 580 nm. After the electron transfer (Figure 2), an oxidized sulfur radical species is released into solution and reacts further to produce MSA and hydroperoxy/superoxide radical ($HO_2^{\cdot}$/$O_2^{\cdot-}$). Two $HO_2^{\cdot}$ disproportionate to H_2O_2 and O_2 [*Stumm and Morgan*, 1996], which explains the concurrent increase in H_2O_2, analogous to the iron-oxalate system [*Pehkonen et al.*, 1993; *Zuo and Hoigné*, 1992]. The reduced iron is detached from the solid surface in a slow step and is then oxidized by H_2O_2, $OH^{\cdot}$, or O_2. Newly formed Fe(III) precipitates as ferrihydrite, as verified by XRD scans of the product. MSA accumulates in solution, being 2 to 3 orders of magnitude more stable with regard to $OH^{\cdot}$ oxidation compared to both DMSO and MSIA [*Bardouki et al.*, 2002; *Zhu et al.*, 2003], and SO_4^{2-} is not observed in any of the experiments.

[12] This surface-controlled dissolution mechanism also explains the initial inhibition of Fe(II) production with DMSO. DMSO is likely to adsorb to the surface of ferrihydrite, thus lowering surface induced $FeOH^{2+}$ photolysis seen in the control experiment. Once MSIA is formed from DMSO oxidation with $OH^{\cdot}$ it partakes in the Fe(III)-MSIA LMCT. In experiments with additions of both MSIA and DMSO, initial rates of Fe(II) production were identical to the experiment with only MSIA, indicating that MSIA readily binds to the ferrihydrite even in the presence of DMSO.

[13] To further investigate the effect of light it was turned off after 6 hours. Results are plotted in Figure 1 in the shaded portion of Figure 1. Since the MSIA is consumed by the time the radiation source is removed in the Fe-MSIA

experiment, only a leveling off of all the products is observed. However, in the case of the DMSO experiment with more UVR, significant changes occur. The production of MSIA radical ceases the moment the radiation source is removed thus prohibiting the subsequent formation of $HO_2^{\cdot}/O_2^{\cdot-}$ and H_2O_2. The short burst in MSIA and MSA concentrations (Figure 1b) may be due to the efficient scavenging of remaining $OH^{\cdot}$ by the abundant DMSO in solution, and the simultaneous Fe(II) increase is presumably due to a combination of two processes: (i) the slow detachment of the already reduced iron from the surface and (ii) the loss of photooxidants, i.e., $HO_2^{\cdot}/O_2^{\cdot-}$, H_2O_2 and $OH^{\cdot}$.

5. Conclusions

[14] These findings suggest a novel and efficient mechanism by which phytoplankton can actively increase the dissolution of iron within acidic aerosol particles in the marine atmosphere by emitting DMS when under oxidative stress, such as iron limitation [*Sunda et al.*, 2002; *Zhuang et al.*, 1992]. The key reaction identified here leads to the dissolution of ferrihydrite by photolysis of the Fe(III)-MSIA complex and does not depend on the production of protons from DMS oxidation. Although such acidification of the particle due to DMS oxidation could potentially enhance iron dissolution [*Zhuang et al.*, 1992], this process has not been substantiated experimentally.

[15] The proposed mechanism between Fe(III) and MSIA remains to be tested in the field, and if found to occur, implications would reach beyond the immediate photochemical increase in Fe(II). The continuous re-processing of iron as part of this mechanism leads to precipitation of kinetically more labile colloidal amorphous iron(oxy)hydroxide that increases the bioavailability of iron [*Waite*, 2001]. Another salient implication of this mechanism impacts the marine sulfur cycle. Oxidation of DMS is thought to lead to new CCN, thus reducing incoming solar radiation [*Charlson et al.*, 1987]. However, this climate feedback postulation is affected by processes, such as that identified here, that lead to the efficient uptake of DMSO into the condensed phase of the aerosol particles and to aqueous phase DMSO oxidation. The resulting reduction in gas phase DMSO lowers the SO_2 product yield and the number of CCN [*von Glasow and Crutzen*, 2004]. Finally, the Fe-MSIA photochemical reaction may offer an efficient and missing source of aqueous MSA in marine sulfur chemistry models [*Lucas and Prinn*, 2002; *von Glasow and Crutzen*, 2004] and help constrain models of iron speciation and solubility over oceans [*Hand et al.*, 2004].

[16] **Acknowledgments.** This research was funded by the National Science Foundation, National Park Service, and Central Washington University. We thank T. Melbourne for careful proofreading of the manuscript.

References

Barbeau, K., and J. W. Moffett (2000), Laboratory and field studies of colloidal iron oxide dissolution as mediated by phagotrophy and photolysis, *Limnol. Oceanogr.*, *45*(4), 827–835.

Bardouki, H., M. B. da Rosa, N. Mihalopoulos, W. U. Palm, and C. Zetzsch (2002), Kinetics and mechanism of the oxidation of dimethylsulfoxide (DMSO) and methanesulfinate (MSI-) by OH radicals in aqueous medium, *Atmos. Environ.*, *36*(29), 4627–4634.

Charlson, R. J., J. E. Lovelock, M. O. Andreae, and S. G. Warren (1987), Oceanic phytoplankton, atmospheric sulphur, cloud albedo and climate, *Nature*, *326*, 655–661.

Chen, Y., and R. L. Siefert (2004), Seasonal and spatial distributions and dry deposition fluxes of atmospheric total and labile iron over the tropical and subtropical North Atlantic Ocean, *J. Geophys. Res.*, *109*, D09305, doi:10.1029/2003JD003958.

Coale, K. H., et al. (1996), A massive phytoplankton bloom induced by an ecosystem-scale iron fertilization experiment in the equatorial Pacific Ocean, *Nature*, *383*, 495–500.

Duce, R. A., and N. W. Tindale (1991), Atmospheric transport of iron and its deposition in the ocean, *Limnol. Oceanogr.*, *36*(8), 1715–1726.

Field, C. B., M. J. Behrenfeld, J. T. Randerson, and P. G. Falkowski (1998), Primary production of the biosphere: Integrating terrestrial and oceanic components, *Science*, *281*, 237–240.

Hand, J. L., N. M. Mahowald, Y. Chen, R. L. Siefert, C. Luo, A. Subramaniam, and I. Fung (2004), Estimates of atmospheric-processed soluble iron from observations and a global mineral aerosol model: Biogeochemical implications, *J. Geophys. Res.*, *109*, D17205, doi:10.1029/2004JD004574.

Johansen, A. M., R. L. Siefert, and M. R. Hoffmann (2000), Chemical composition of aerosols collected over the tropical North Atlantic Ocean, *J. Geophys. Res.*, *105*(D12), 15,277–15,312.

Lucas, D. D., and R. G. Prinn (2002), Mechanistic studies of dimethylsulfide oxidation products using an observationally constrained model, *J. Geophys. Res.*, *107*(D14), 4201, doi:10.1029/2001JD000843.

Martin, J. H., and S. F. Fitzwater (1988), Iron deficiency limits phytoplankton growth in the north-east Pacific subarctic, *Nature*, *331*, 341–342.

Moffett, J. W. (2001), Transformations among different forms of iron in the ocean, in *The Biogeochemistry of Iron in Seawater*, edited by D. R. Turner and K. A. Hunter, pp. 344–372, John Wiley, Hoboken, N. J.

Pehkonen, S. O., R. Siefert, Y. Erel, S. Webb, and M. Hoffmann (1993), Photoreduction of iron oxyhydroxides in the presence of important atmospheric organic compounds, *Environ. Sci. Technol.*, *27*(10), 2056–2062.

Schwertmann, U., and R. M. Cornell (1991), *Iron Oxides in the Laboratory, Preparation and Characterization*, John Wiley, Hoboken, N. J.

Sciare, J., E. Baboukas, M. Kanakidou, U. Krischke, S. Belviso, H. Bardouki, and N. Mihalopoulos (2000), Spatial and temporal variability of atmospheric sulfur-containing gases and particles during the Albatross campaign, *J. Geophys. Res.*, *105*(D11), 14,433–14,448.

Shaked, Y., A. B. Kustka, and F. M. M. Morel (2005), A general kinetic model for iron acquisition by eukaryotic phytoplankton, *Limnol. Oceanogr.*, *30*(3), 872–882.

Stookey, L. L. (1970), Ferrozine—A new spectrophotometric reagent for iron, *Anal. Chem.*, *42*(7), 779–781.

Stumm, W., and J. J. Morgan (1996), *Aquatic Chemistry*, John Wiley, Hoboken, N. J.

Sunda, W. (2001), Bioavailability and bioaccumulation of iron in the sea, in *The Biogeochemistry of Iron in Seawater*, edited by D. R. Turner and K. A. Hunter, pp. 41–84, John Wiley, Hoboken, N. J.

Sunda, W., D. J. Kieber, R. P. Kiene, and S. Hunstman (2002), An antioxidant function for DMSP and DMS in marine algae, *Nature*, *418*, 317–320.

Voelker, B. M., and D. L. Sedlak (1995), Iron reduction by photoproduced superoxide in seawater, *Mar. Chem.*, *50*, 93–102.

von Glasow, R., and R. Sander (2001), Variation of sea salt aerosol pH with relative humidity, *Geophys. Res. Lett.*, *28*(2), 247–250.

von Glasow, R., and P. J. Crutzen (2004), Model study of multiphase DMS oxidation with a focus on halogens, *Atmos. Chem. Phys.*, *4*, 589–608.

Waite, D. T. (2001), Thermodynamics of the iron system in seawater, in *The Biogeochemistry of Iron in Seawater*, edited by D. R. Turner and K. A. Hunter, pp. 292–342, John Wiley, Hoboken, N. J.

Wehrli, B., B. Sulzberger, and W. Stumm (1989), Redox processes catalyzed by hydrous oxide surfaces, *Chem. Geol.*, *78*, 167–179.

Zhu, L., J. M. Nicovich, and P. H. Wine (2003), Temperature-dependent kinetics of aqueous phase reactions of hydroxyl radicals with dimethylsulfoxide, dimethylsulfone, and methanesulfonate, *Aquat. Sci.*, *65*, 425–435.

Zhuang, G., Z. Yi, R. A. Duce, and P. R. Brown (1992), Link between iron and sulphur cycles suggested by detection of Fe (II) in remote marine aerosols, *Nature*, *355*, 537–539.

Zuo, Y., and J. Hoigné (1992), Formation of hydrogen peroxide and depletion of oxalic acid in atmospheric water by photolysis of iron (III)-oxalato complexes, *Environ. Sci. Technol.*, *26*(5), 1014–1022.

A. M. Johansen and J. M. Key, Department of Chemistry, Central Washington University, 400 East University Way, Ellensburg, WA 98926, USA. (johansea@cwu.edu)